Two-phase simulations on transient flow in scroll compressor using VOF method

Jihyun KIM[1], Yanghee CHO[2], Jaesang LEE[2], Hyungmin PARK[1,*]

[1]Seoul National University, Institute of Advanced Machines and Design,
Seoul, Republic of Korea

[2]SAMSUNG ELECTRONICS Co., Energy Technology Lab.,
Suwon-si, Gyeonggi-do, Republic of Korea

*Corresponding Author: hminpark@snu.ac.kr

ABSTRACT

In operating scroll compressors, lubrication oil is in general injected between the moving parts, to cool the working gas or to reduce the gaps between them. However, it is challenging to analyze the two-phase flow in a scroll compressor due to the complicated structure including narrow gaps. We conducted three-dimensional two-phase numerical simulations in the transient flow field in a scroll compressor using R32 as a working fluid and POE85 as a lubricating oil. Oil and refrigerant were modeled using the Volume of Fluid (VOF) method. The refrigerant property tables were generated from REFPROP and during calculation, each thermodynamic property of the refrigerant was interpolated using UDRGM (User-Defined Real Gas Model), thereby reducing the computational time. Bypass valves were included in the scroll compressor geometry and the mesh update during the valve motion occurred using the layering method. Additionally, the deformation of chamber part geometry was simulated using Structured Dynamic Mesh (SDM) method. By implementing these approaches, we could maintain high grid quality and a sufficient number of mesh including the flank gap region. In this paper, we investigated the influence of the oil on the compression performance and local flow field. In the presence of valve motions, a modest reduction in discharge temperature was observed, accompanied by the increase in mass flow rate.

1. INTRODUCTION

The scroll compressor is mainly used in air conditioners due to its remarkable efficiency, which makes it appropriate for various applications such as fuel cell vehicles (FCV) (Zhang *et al*., 2018) and small-scale compressed air energy storage (CAES) (Liu *et al*., 2022, Ma *et al*., 2019). Hence, it is critical to examine the internal flow of the scroll compressor and optimize its geometry to ensure energy conservation and increase efficiency.

Several studies have been carried out to assess the efficiency and improve the structure of scroll compressors using thermodynamic models, computational fluid dynamics, and other techniques. Wang *et al*. (2008) developed a quasi-steady-state model for predicting the performance of scroll compressors incorporating refrigerant injection and experimentally validated the model. In addition to predicting the compressor's overall performance with high accuracy, this mathematical model can also estimate the chamber pressure at various crank angles. Ooi and Zhu (2004) analyzed heat transfer and flow fields inside a scroll compressor using a two-dimensional simulation, employing a two-boundary algebraic method for grid generation. Using a two-dimensional simulation, Morini *et al*. (2015) used Reynolds-Averaged Navier-Stokes (RANS) with Computational Fluid Dynamics (CFD) to examine the internal flow of a scroll compressor. However, these two-dimensional flow analysis methods are incapable of simulating the discharge process that is perpendicular to the chambers. Additionally, they are unable to examine the impact of axial leakage on the flow field. In order to investigate the internal flow of a scroll refrigeration compressor, Sun *et al*. (2017) used a three-dimensional simulation. This analysis provided insight into the mechanisms causing fluctuations in the mass flow rates at the inlet and exit as well as asymmetric pressure distributions.

In this paper, we used POE85 as a lubricating oil and R32 refrigerant as the working fluid to perform three-dimensional simulations to study the flow field inside a scroll compressor. The thermodynamic properties were described in a tabular style with each property expressed as a function of temperature and pressure to improve computational efficiency. We utilized the Structured Dynamic Mesh (SDM) technique, which involves moving the mesh based on projection, aiming for high quality of the grid, particularly in terms of orthogonality.

2. NUMERICAL METHOD

The numerical investigation was conducted using the commercial software Fluent. The working fluid and lubrication oil used were R32 and POE85, respectively. The refrigerant property tables were created using REFPROP. During the calculation, each thermodynamic property of the refrigerant was interpolated using UDRGM (User-Defined Real Gas Model), which allowed reduce the computational time. The oil was characterized as an incompressible fluid with a constant density of 1033 kg/m^3. The Volume of Fluid (VOF) approach was used to model the two-phase flow of oil and refrigerant. The analysis was performed under ARI conditions with and without oil, and pressure inlet and pressure outlet were applied as boundary conditions. Table 1 shows the detailed boundary conditions.

Table 1: Boundary conditions

Case	Inlet			Outlet pressure	Rotational speed
	Pressure	Temperature	Mass fraction of oil		
1	1017.7 [kPa]	291.45 [K]	0	3472.7 [kPa]	3600 [rpm]
2			3%wt		

The rotational speed was set to 3600 rpm, assuming a high rotational velocity, without considering the heat exchange between the wall and the fluid (Sun *et al*., 2017). No-slip conditions were applied to every wall. Due to the swirling motion in the compressor flow, the RNG k-epsilon model was employed.

Figure 1 illustrates the division of the fluid domain into multiple sections, including the chamber part, suction part, bypass ports, bypass valve part, discharge part, and axial gaps located above and below the chamber part. We utilized hexahedral grids for the chamber, suction, bypass ports, bypass valve parts, and axial gaps while employing tetrahedral grids for the discharge part. To accurately analyze the flow field in a scroll compressor, it is important to realize the shape change with respect to the crank angle due to the movement of the orbiting scroll. By applying the structured dynamic mesh method provided by Wang *et al*. (2015), it was possible to maintain the number of mesh components across flank gaps at a constant value of 10. Through modification of the node movement equation as indicated by Equations (1) and (2), we successfully improved the mesh quality, including the flank gap region (Figure 2). The process of updating the node positions began with the intermediate layer to ensure optimal performance, even in a central location with large curvature.

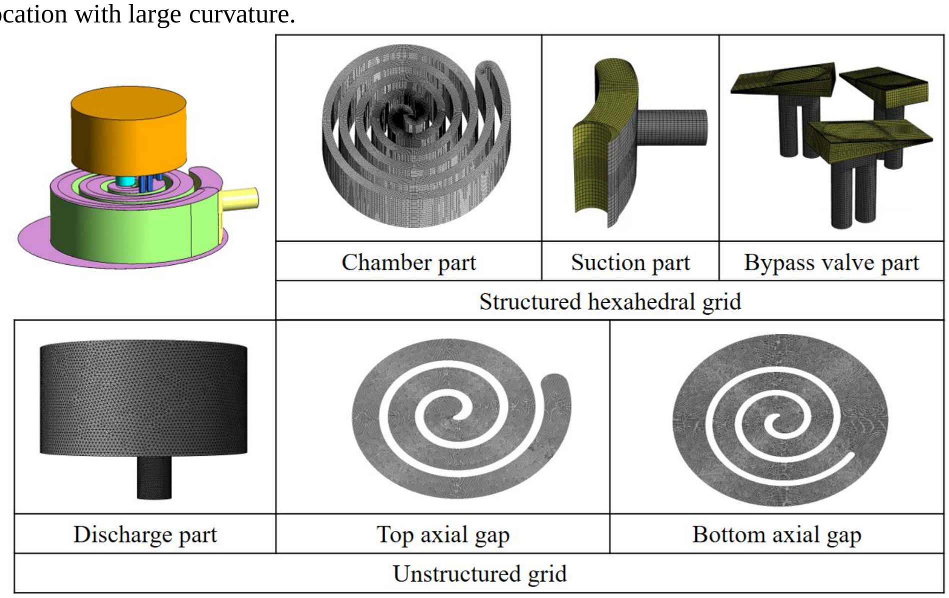

Figure 1: Grids for fluid domains

$$\overrightarrow{X_i X_{iprevious}} \cdot \vec{T} < \varepsilon \quad (1)$$
$$\overrightarrow{X_i X_{iprevious}} = X_i - X_{i-previous} \quad (2)$$

Here, subscription i is an index of each layer, X is a node coordinate, $\vec{T}$ is a tangential vector of the previous layer and ε is threshold value respectively. All node positions in the chamber part were calculated every 0.5 degree of crank angle in advance and saved in text format using MATLAB. At the beginning of each time-step, corresponding node information file was read and node update occurred via UDF (user-defined function).

Reed valves are commonly used as bypass valves in lower compression ratios to prevent over-compression. Once the internal pressure surpasses the discharge pressure, the bypass valve will bend allowing the refrigerant to be discharged through the bypass port. Fluid-structure interaction (FSI) analysis is necessary for simulating bending motion, but it requires an incredibly short time-step size because of the bypass valve's extremely small inertia. In this study, the bypass valve motion was simplified to rigid body rotation assuming torsional mass and spring system (Figure 3a). The torsion coefficient κ was properly determined using Equation (3) as described by Ding and Gao (2014).

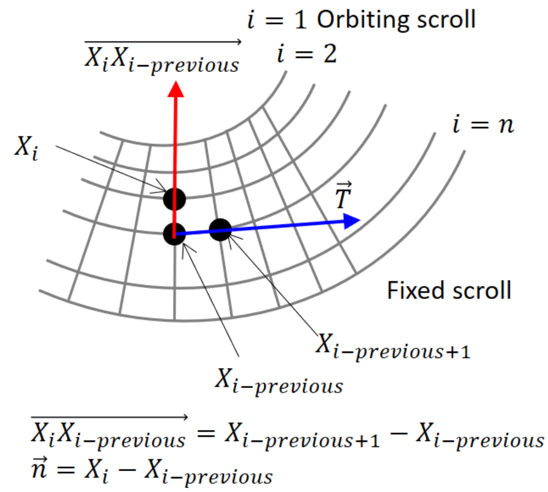

Figure 2: Schematic of grid update

$$\kappa = \frac{\tau}{\theta} = \frac{Pa^2}{y} = \frac{3EI}{a} \quad (3)$$

Here, τ is the torque from fluid force, θ is the angle of the valve, P is concentrated force, a is the distance between the fixed end and a center line of bypass port, y is deflection, E, and I are elastic modulus of the bypass valve and the area moment of inertia respectively. Mesh deformation induced by the valve movement was addressed using layering technique (Figure 3b).

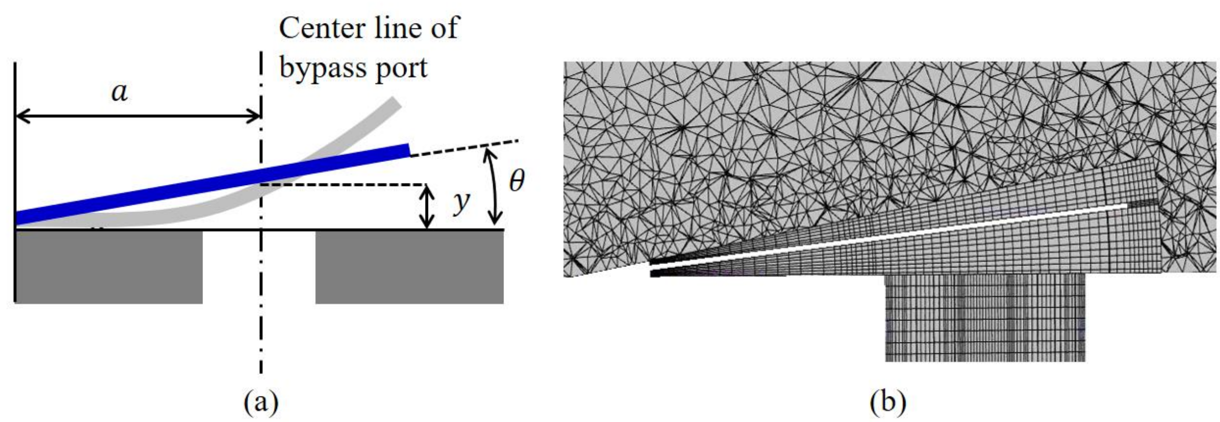

Figure 3: Schematic of bypass valve model (a), mesh for bypass valve part (b)

3. RESULTS

This simulation focused on investigating the impact of lubricating oil. Figure 4 displays the oil volume fraction for crank angles of 0° and 120°. The oil volume fraction is found to be higher in the central chamber under higher pressure. In addition, the two compression pathways have different crank angles at which the compression process starts because of the asymmetrical structure of the scroll compressor. This leads to an uneven distribution of the volume fraction.

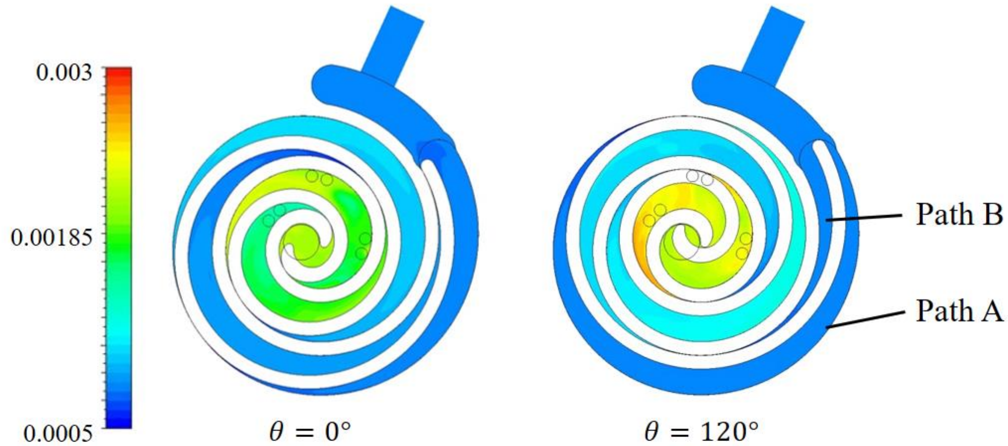

Figure 4: Oil volume fraction at the crank angle of 0° and 120°

Figure 5 depicts the velocity distribution at the axial gaps located at the top and bottom. Figures 5(a) and (b) correspond to the case of two-phase flow, whereas Figures 5(c) and (d) simulate the single-phase flow case. The two-phase flow case, which contains oil, shows decreased leakage velocity at the top axial gap (Figures 5(a) and (c)). Similarly, the bottom axial leakage is also reduced in the two-phase flow case as shown in Figures 5(b) and (d).
The chamber temperatures in Figures 6(a) and (b) for the two-phase flow case, and Figures 6(c) and (d) for the single-phase flow case, respectively, are displayed. In the case involving lubrication oil, the oil serves to improve cooling and reduce leakage through the axial gaps, resulting in decreased temperatures. This decrease in leakage can also be detected in the pressure curve.

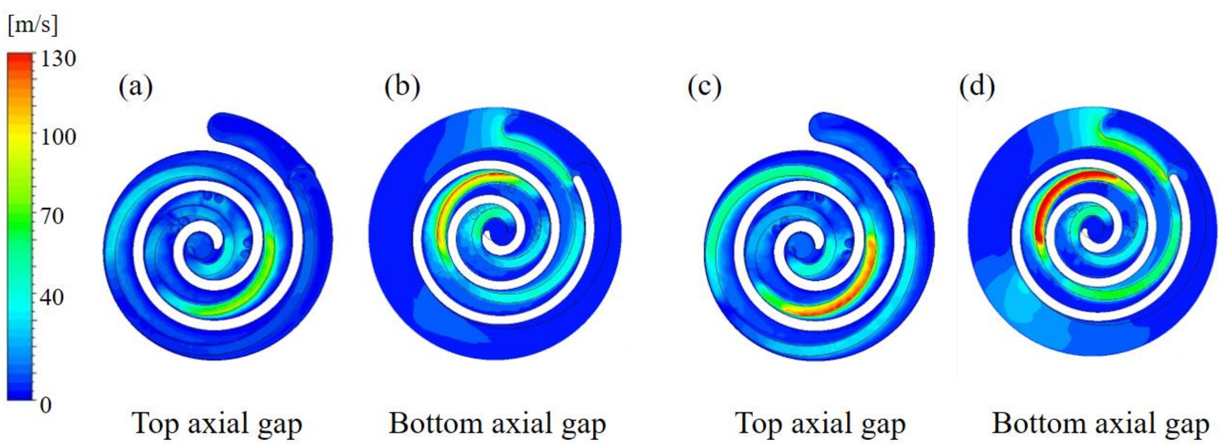

Figure 5: Velocity distribution at the top and bottom axial gap; two-phase case (a), (b), single-phase case (c), (d)

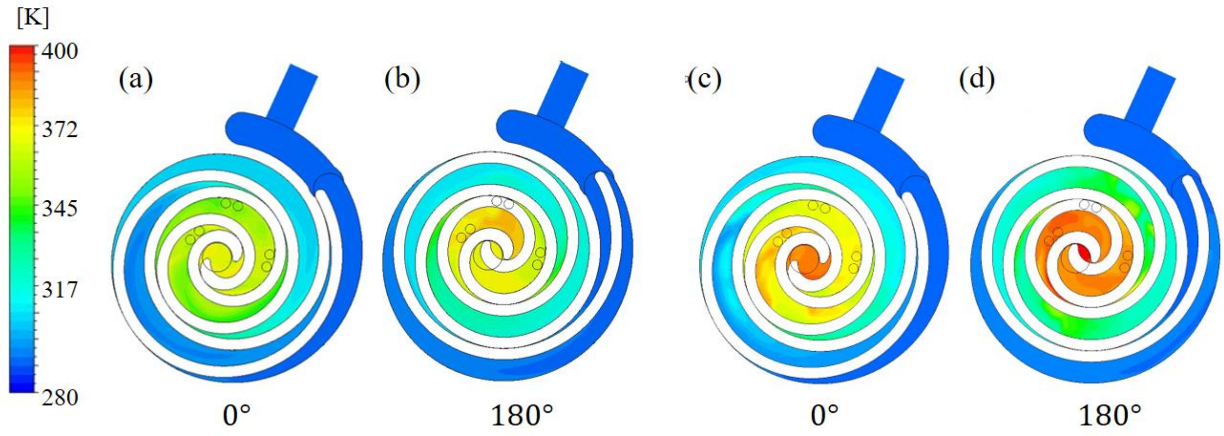

Figure 6: Temperature distribution in compression chambers; two-phase case (a), (b), single-phase case (c), (d)

Figures 7(a) and (b) demonstrate the compression operations through Paths A and B, respectively. Compression starts at 180°in Path A and 360° in Path B. Yet, as a result of pre-compression, the pressure at 180° in Path A and 360° in Path B is slightly greater than the suction pressure at these specific angles. This phenomenon occurs when high-pressure refrigerant flows into the following chamber as the gap between the orbiting scroll and the fixed scroll becomes smaller. This occurs less in the two-phase case represented by the red line compared to the black line of the single-phase case. Following the suction process, the pressure curve of the two-phase case shows a lower slope compared to the single-phase case. The single-phase case reaches the discharge pressure faster, beginning the discharge process at 786° and 810° in Paths A and B, respectively. In contrast, the two-phase case starts the discharge process at 807° and 839°.

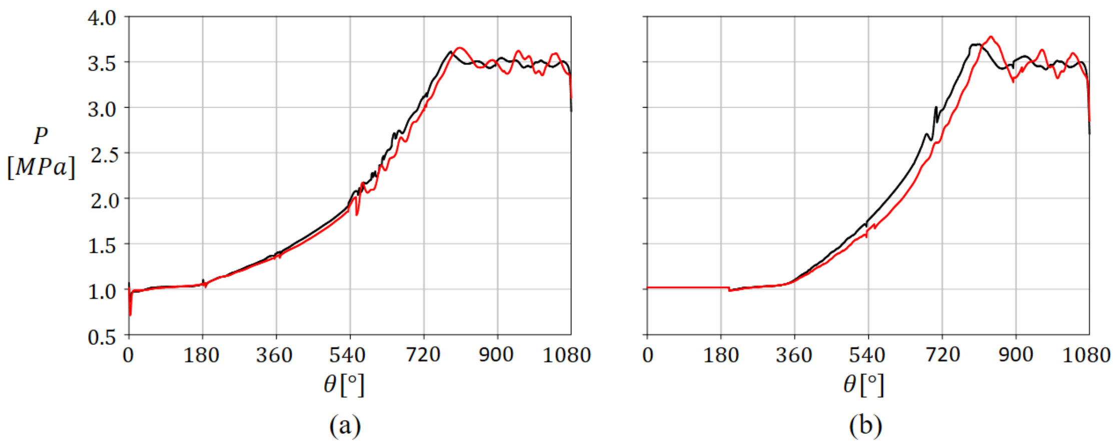

Figure 7: Compression process through the path A (a), path B (b); — : two-phase case, — : single-phase case

4. CONCLUSIONS

This study investigated the influence of lubrication oil on a two-phase scroll compressor, specifically analyzing how the presence of oil affects temperature and leakage velocity. The results of our study indicate that the use of oil greatly improves the cooling process and decreases the amount of leakage via the axial gaps, resulting in a lower temperature distribution within the chamber. This is obvious from the pressure curves, which also demonstrate decreased leakage. Regarding the pressure curve, pre-compression results in a slight elevation of pressure at suction angles (180 degrees in Path A and 360 degrees in Path B), surpassing the suction pressure at these crank angles.

REFERENCES

Ding, H., & Gao, H. (2014). 3-D Transient CFD Model For A Rolling Piston Compressor With A Dynamic Reed valve.
Liu, Z., Li, Z., Xie, D., & Wu, H. (2022). Unsteady characteristic and flow mechanism of a scroll compressor in small-scale compressed air energy storage system. Journal of Energy Storage, 51, 104368.
Ma, X., Zhang, C., & Li, K. (2019). Hybrid modeling and efficiency analysis of the scroll compressor used in micro compressed air energy storage system. Applied Thermal Engineering, 161, 114139.
Morini, M., Pavan, C., Pinelli, M., Romito, E., & Suman, A. (2015). Analysis of a scroll machine for micro ORC applications by means of a RE/CFD methodology. Applied Thermal Engineering, 80, 132-140.
Ooi, K. T., & Zhu, J. (2004). Convective heat transfer in a scroll compressor chamber: a 2-D simulation. International Journal of Thermal Sciences, 43(7), 677-688.
Sun, S., Wu, K., Guo, P., & Yan, J. (2017). Analysis of the three-dimensional transient flow in a scroll refrigeration compressor. Applied Thermal Engineering, 127, 1086-1094.
Wang, B., Shi, W., Li, X., & Yan, Q. (2008). Numerical research on the scroll compressor with refrigeration injection. Applied Thermal Engineering, 28(5-6), 440-449.
Wang, J., Song, Y., Li, Q., & Zhang, D. (2015). Novel structured dynamic mesh generation for CFD analysis of scroll compressors. Proceedings of the Institution of Mechanical Engineers, Part A: Journal of Power and Energy, 229(8), 1007-1018.
Zhang, Q., Feng, J., Wen, J., & Peng, X. (2018). 3D transient CFD modelling of a scroll-type hydrogen pump used in FCVs. International Journal of Hydrogen Energy, 43(41), 19231-19241.

ACKNOWLEDGEMENT

This work was supported by Samsung Electronics, Korea.